Desalination and Water Treatment
www.deswater.com

doi:10.5004/dwt.2019.23742

148 (2019) 270–284
April

Removal of Cr(VI) from aqueous media on calcined (Mg-Zn)/(Al-Fe)-(CO_3)/Cl layered double hydroxides

Medhat A.H. Hafez[a,#], Ibrahim M.M. Kenawy[a], Zaynab M.E. Abd Elbary[a,*], Randa R. Elmorsi[b], Khaled S. Abou-El-Sherbini[c]

[a]*Department of Chemistry, Faculty of Science, Mansoura University, Mansoura 35516, Egypt, email: ibrahimkenawy45@gmail.com (I.M.M. Kenawy); isis_eg@yahoo.com (Z.M.E.A. Elbary),*
[b]*National Institute of Oceanography and Fisheries, Suez branch, Adabiyah-Suez road, Attaqa district, Suez, Egypt, email: rrelmorsi@hotmail.com (R.R. Elmorsi)*
[c]*Department of Inorganic Chemistry, National Research Centre, 33 El Bohouthst. (former Tahrir st.), 12622, Dokki, Giza, Egypt, email: kh_sherbini@yahoo.com (K.S. Abou-El-Sherbini)*

Received 15 July 2018; Accepted 1 January 2019

ABSTRACT

The three newly reported calcined layered double hydroxides (CLDHs) coded CLDH10, CLDH21 and CLDH22 were synthesized by co-precipitation method. The characterization of CLDHs before and after loading with CrO_4^{2-} with Fourier transform infrared (FTIR), scanning electron microscope (SEM), electron dispersive X-ray analysis (EDX) and flame atomic absorption spectrometry (FAAS) showed a typical hydrotalcite structure and confirmed the loading of Cr(VI). The sorption process of Cr(VI) as chromate was investigated onto these CLDHs using batch method. The sorption parameters; initial pH, shaking time, sorbent dose, initial concentration of chromate and temperature were studied. The optimum conditions for Cr(VI) sorption were obtained at initial pH 7.1, sorbent dose 25 mg and shaking time 3 h. The complete removal of 50 mg L^{-1} of chromate (>99%) was achieved at sorbent dosage ≥ 50 mg (0.2% w/v) of CLDH sorbents. The sorption process was suggested to follow the pseudo-second-order kinetics and Langmuir-type isotherm with monolayer capacities 40.0, 38.5 and 52.6 mg g^{-1}, onto CLDH10, CLDH21 and CLDH22, respectively. The measured thermodynamic parameters ΔG_{ads}, ΔH_{ads} and ΔS_{ads} indicated that the sorption process was spontaneous and endothermic in nature. The loaded chromate was best recovered from CLDH sorbents using 1.0 mol L^{-1} Na_2CO_3. CLDH22 showed best sorption capacity (45.7 mmol/100 g) with possible magnetic separation. It was applied successfully for the removal of Cr(VI and III)from standard reference material, tanning effluents,leather scraps and cement extract with removal efficiencies of 88.5–100%.

Keywords: Calcined layered double hydroxides; Sorption; Cr(VI); Wastewater treatment

---

1. Introduction

The environmental pollution with heavy metals from many industries is a significant problem owing to their hazardous effects on human health and environment even at low concentrations [1]. Chromium, in particular, is one of the most dangerous inorganic water pollutants that released by natural processes and by anthropogenic sources such as tanning industry [2]. The hexavalent form is highly mobile and toxic due to its carcinogenic and mutagenic nature. It is highly mobile in soil and aquatic system and also a strong oxidant capable of being absorbed by the skin. Hence, effluents or water contaminated with chromium(VI) must be treated before discharge [3–6].

Several recent treatment methodologies and technologies are being applied to remove chromium ions such as coagulation, membrane separation, nanofiltration, solid phase extraction (SPE) and biological treatment [7–10]. However,

---

*Corresponding author.

[#]*Dedicated to* ***Prof. Dr. Medhat A.H. Hafez*** *who deceased on November 15, 2017.*

1944-3994 / 1944-3986

most of these techniques have limitations of high cost, low efficiency, production of sludge, non-recoverability and inapplicability to a wide range of pollutants and/or the generation of secondary pollution. SPE arose as a conventional technique and highly efficient physico-chemical treatment process for the removal of inorganic pollutants from their aqueous and sometimes gaseous matrices [8,10,11]. The main advantages of this technique are its greater flexibility in the design of the aimed sorbent for the target pollutant, high efficiency, reusability of material, easy handling and inexpensive [11,12].

Layered double hydroxides (LDHs) are one of the most important two-dimensional layered SPE sorbents with a brucite-like $M^{2+}_{(1-x)}/M^{3+}_{x}$ structure intercalated with anions (x/n A^{n-}) for charge compensation [13–15]. Their derivative materials have also attracted multidisciplinary attention due to the unique advantages of their moderate chemiostability, potentially cheap sorbents with high anion-exchange capacity. They are also easily synthesized, selective,regenerative and nontoxicity so, they are eco-friendly structure [16].Their calcination products (CLDHs) restore the LDH structure, once being hydrolysed, with larger surface area and better sorption efficiency [17]. As well as, CLDHs have enabled massive developments in effective pollution treatments. Over the past few decades, significant advances have been made in the synthesis of novel LDH-based composites and the optimization of characterization techniques. Many studies reported the use of LDHs and in particular CLDHs for Cr(VI) separation [18–26]. Zn/Al and Fe_3O_4/Zn/Al CLDHs were used for Cr(VI) with maximum uptake 10.9 and 9.95 mmol/100 g, respectively [23]. Also, calcined Zn/Al and Zn/Al/Cr with ratio (4:1) were used for the Cr(VI) removal with maximum sorption capacity 24.3 and 9.31 mmol/100 g, respectively [24]. In addition, Mg–Zn/Al LDH and CLDH were employed for Cr(VI) with sorption capacity of 13.5 and 15.7 mmol/100 g, respectively [25]. Furthermore, Mg/Al, Ni/Al and Zn/Al LDHs were synthesized with molar ratio ($M^{2+}/M^{3+} = 3$). Their maximum capacities were 14.0, 26.6 and 31.5 mmol/100 g, respectively [26]. Additionally, Mg/Al LDHs (2:1) with NO_3^-, Cl^- and SO_4^{2-} as interlayer anion were reported to adsorb Cr(VI) with maximum capacities 33.3, 27.2 and 25.7 mmol/100 g, respectively [27]. Chromium(VI) was sorbed on calcined graphene/MgAl-LDH with maximum sorption capacity 3.72 mmol/100 g [28]. The nanoscale zero-valent iron (NZVI) was used for Cr(VI) removal with capacity 43.9 mg/g [29]. As well as, the porous metal-organic frameworks (MOFs) were employed to absorb Cr(VI) with capacity (37–68.5) mg/g [30]. Also, in the review by Zhao et al. [31], Polyacrylonitrile/polypyrrolecore/shell nanofiber (PPy), magnetic cyclodextrin–chitosan/GO and cellulose-sodium montmorillonite were used to remove Cr(VI) with capacity (61.8, 61.31, 22.2 mg/g), respectively. Major challenges for the sorption of Cr(VI) on LDH are to overcome its preference of anions with the order $NO_3^- < Cl^- < OH^- < SO_4^{2-} < CO_3^{2-}$ [13], enhance its sorption capacity and acquiring reasonable kinetics [19] while maintaining the chemical stability.

The LDH stabilities were reported to increase when $x \approx 0.25$, and in the presence of Zn (II) or Fe(III) in its structure [14,15]. Cl^- containing LDHs appear to be among the best precursors for ion exchange reactions [13].

Recently, a series of LDH compositions of (Mg, Zn)/(Al, Fe)-(CO_3, Cl) was synthesized which gave promising sorption capacities with magnetic properties for an ionic hazards [32]. Although, CLDHs coded CLDH10, CLDH21 and CLDH22 showed promising sorption behavior towards Cr(VI), their sorption behavior has not studied yet in detail. The present work is carried out to optimize the parameters affecting the sorption process of Cr(VI) on these CLDHs in order to enhance their removal efficiency. Also, the process will be applied for the removal of total Cr(III&VI) from polluted samples.

2. Materials and methods

2.1. Materials

The materials used in the synthesis of layered double hydroxides (LDHs) were of analytical grade. Magnesium chloride ($MgCl_2$), zinc chloride ($ZnCl_2$, 97%), aluminum chloride ($AlCl_3 \cdot 6H_2O$, 97%), ferric chloride ($FeCl_3$, 98%), NaOH and Na_2CO_3 were obtained from ALPHA CHEMIKA, Mumbai-India, and were used as received. Potassium chromate was obtained from Merck. Chromium removal at optimized conditions was performed on tanning leather scraps and tanning effluents (A and B). The tanning effluents are spent chromate treatment solutions gathered from two different tanning factories. Commercial Portland and white cement samples were purchased from the market for application. The Cr standard reference material of, number 835018 from High-Purity Standards, Charleston, SC, USA was used for the separation process validation.

2.2. Synthesis of the sorbents

The synthesis procedure was followed as previously described [32] and detailed in S1 to obtain LDH10, LDH21 and LDH22 and their calcined products CLDH10, CLDH21 and CLDH22, respectively. The proportion of salts used for the synthesis of LDHs and their codes are in Table 1.

2.3. Micro-structural and mineralogical characterization

Fourier transform infrared (FTIR) spectra were recorded on a Nicolet iS10, Thermo-Fisher Scientific, USA, using KBr pellets. Specific surface area (S_{BET}) was determined with a BELSORP-mini II, BEL Japan, INC, using nitrogen at 77 K.

Table 1
Proportion of salts used for the synthesis of LDHs and their codes

Sample code	Initial molar chloride solutions Mg/Zn/Al/Fe ratio	Final Mg/Zn/Al/Fe/Cl/CO_3 ratio
LDH10	2.7/0.3/1/0	3.67/0.26/1.00/0/0.55/0.22
LDH21	2.4/0.6/0.9/0.1	2.72/0.72/0.80/0.20/0.26/0.37
LDH22	2.4/0.6/0.8/0.2	2.30/0.56/0.74/0.26/0.29/0.35

Prior to measurement, the sorbents were heated at 105 and 450°C for LDH22 and CLDH22, respectively, in a vacuum for 12 h to remove surface contaminants and sorbed water. The scanning electron microscope (SEM) images were performed using SEM model Quanta 250 FEG (Field Emission Gun) with accelerating voltage 30 K.V., magnification 14 xs up to 10^6 and resolution for Gun. 1n, FEI Company, Netherlands, after covering with gold (except for LDH22). Electron dispersive X-ray analysis (EDX) was carried out for uncovered samples on Oxford X-Max 20 model.

UV-visible absorption spectrometric measurements were recorded on NUICO 1200 (USA) using a 1 cm quartz cell. The final concentration of the chromate solution was measured by UV-Vis spectrometry at a wavelength of 366 nm [33]. Standard chromate solution of known concentration was prepared in the range 2–30 mg L^{-1}, which give a linear calibration curve. A blank sample containing no chromate and another containing chromate solution were measured together with every batch of sample run.

The chemical composition of the contaminated real samples (given in Table 2), was assessed and detailed in S2.

The point zero charge (pH_{PZC}) of CLDH sorbents was determined by the adjustment of initial pH of 0.1 M NaCl solutions to a pH range of 2–12, as described in S3.

2.4. Preparation of the stock solutions

The chromate stock solution was prepared by dissolving accurately weighed chromate (as potassium chromate) in bi-distilled water to a concentration of 1000 mg L^{-1}. The sample solution was obtained by appropriate dilutions to different initial concentrations. The Cr standard reference material was slowly dissolved in HCl in open air to prepare a stock 1000 mg L^{-1} of Cr(III).

All measurements were performed in triplicate runs.

2.5. Optimization of sorption parameters

2.5.1. Sorption experiments

CLDH10, CLDH21 and CLDH22 were tested as sorbents for chromate ions (CrO_4^{2-}) using batch-mode experiments at 30°C. Typically, 25 mg of CLDHs was shaken for 3 h in 25 mL of chromate solution with an initial concentration 30 mg L^{-1}. The effect of initial pH was studied within the range 4.33–10.5. The suspensions were left for 24 h to ensure equilibration, centrifuged and the residual chromate concentration in the clear solution was measured spectrophotometrically.

To study the effect of shaking time, 25 mg of each sorbet was suspended in 25 mL of the chromate solution with an initial concentration 15 mg L^{-1}, at the optimum initial pH 7.1, which resulted from the pH study and the final concentration was measured at different time intervals 30–1440 min. The same experiment was repeated in case of CLDH22 at initial chromate concentration of 25 mg L^{-1}.

Effect of sorbent dose on the sorption of 25 mL of chromate was performed by applying doses 12.5–150 mg of different sorbents with an initial concentration 50 mg L^{-1} of chromate solution, at pH 7.1. Then the suspensions were shaken for 3 h, centrifuged after 24 h and the residual concentration was measured.

Effect of initial concentration was studied by suspending 25 mg of CLDHs with 25 mL of chromate with an initial concentrations 15–55 mg L^{-1}, at the optimum initial pH. The suspensions were then shaken for 3 h, and the final chromate solution was centrifuged after 24 h.

Effect of temperature was similarly studied for CLDH22, by suspending 25 mg of the sorbent with 25 mL of chromate solution at pH 7.1 with an initial concentration 55 mg L^{-1}, at different temperatures 20–40°C in thermostated baths. Then the suspensions were shaken for 3 h, centrifuged after 24 h and the residual chromate concentration was measured.

Sorption capacity (q_e) of chromate onto CLDHs at equilibrium (q_e, mg g^{-1}) was calculated using Eq. (1):

$$q_e = \frac{(C_i - C_e)}{m}\ V\ (mg / g) \tag{1}$$

C_i and C_e are the liquid-phase, initial and equilibrium concentrations (mg L^{-1}) of chromate. V is the volume of solution (L) and m is the mass of sorbent (g).

The removal efficiency, R (%), was calculated using Eq. (2):

$$R(\%) = \frac{(C_i - C_e)}{C_i}\ \times 100\ (\%) \tag{2}$$

2.5.2.Removal of Cr(III) after preliminary oxidation

A standard 1000 mg L^{-1} of Cr(II) was oxidized by H_2O_2 in basic medium and boiled to complete oxidation and

Table 2
Analysis of the contaminated real samples

Sample	pH	EC (mS cm^{-1})	Na (g L^{-1})	K (g L^{-1})	Mg (g L^{-1})	Ca (g L^{-1})	Cl (g L^{-1})	SO_4 (g L^{-1})
Tanning effluent (A)	3.11	315	75.8	0.05	ND	ND	63.6	1.66
Tanning effluent (B)	2.27	131	3.14	0.002	ND	ND	18.7	ND
Tanned leather scraps (extract)	0.44	87.0	15.8	0.19	ND	ND	18.2	9.56
White cement* suspension	12.6	30.2	3.18	0.92	0.75	3.93	1.17	17.3
Portland cement* suspension	12.5	39.6	2.23	1.63	0.23	2.40	1.17	11.8

ND = not detected.

removal of excess H_2O_2 [34] then the removal procedure described above for Cr(VI) was followed after proper dilution to approach a chromate concentration of 50 mg L^{-1} onto CLDH22 at optimum conditions.

2.5.3. Examination of kinetic models

The experimental sorption time data obtained was used in the four simplified kinetic equations form as described in S4.

2.5.4. Fitting of sorption isotherm models

The Langmuir's, Freundlich's and Redlich-Peterson models are applied for describing uptake as detailed in S5.

2.5.5. Determination of the thermodynamic parameters

The thermodynamic parameters of sorption were calculated using Van't Hoff's equation (S6):

2.6. Desorption study

For desorption studies, 25 mg of CLDHs was loaded with chromate applying the sorption parameters: an initial concentration (C_i) 30 mg L^{-1} in 25 mL, pH 7.1, time of shaking 3 h, and centrifuged after 24 h. Then the precipitates were collected, washed with bi-distilled water and dried at 50°C. The residual concentration (C_f) in the supernatant liquors was determined after centrifugation. After that, the precipitate (coded CLDHsL) was either characterized by FTIR and SEM-EDX or stirred in 25 mL of solution containing 0.1 M NaCl, 0.1 M NaOH, 0.1 M or 1.0 M Na_2CO_3 for 30 min at 30ºC.

The released chromate concentration (C_R) was measured spectrophotometrically and the recovery efficiency, E (%), was calculated by Eq. (3):

$$E(\%) = \frac{C_R}{C_i - C_f} \times 100\ (\%) \tag{3}$$

2.7. Removal of Cr(III and VI) at optimized conditions

The removal of Cr(III&VI) species from some contaminated samples were targeted either by direct loading on or after preliminary oxidation, respectively.

For tanning effluents (A and B), first the removal of Cr(VI) was performed by adding 25 mg of CLDH22 to 25 mL of each of the tanning effluents at pH 7.1. Then, suspensions were shaken for 3 h, centrifuged after 24 h and the final concentration was measured by FAAS. For the removal of total Cr(III&VI) in 25 mL of the effluent sample, Cr(III) was oxidized by H_2O_2 in basic medium, then the removal procedure of Cr(VI) was followed after proper dilution of 50 mg L^{-1}.

For scraps of tanning leather, 2 g of the sample was digested in 10 mL of concentrated HCl for 24 h, then filtered and the filtrate was adjusted to a volume of 100 mL. Then, the removal procedure described above for tanning effluents was followed on 25 mL.

For cement sample, 50 g of the sample was shaken in 50 mL distilled water for 10 min, and then filtered and the filtrate was adjusted to 50 mL. After that, the removal procedure described above for tanning effluents was followed on 25 mL. The removal efficiency, R (%), was calculated using Eq. (2).

3. Results and discussion

3.1. Micro-structural characterization

The LDHs LDH10, LDH21 and LDH22 were previously characterized by powder X-ray diffraction, thermogrvimetric analysis and FTIR [32]. The layered structure of hydrotalcite-like structures was confirmed of which its Van der Waal's gaps were lost upon calcinations due to the formation of the corresponding oxides.

3.1.1. FTIR

Fig. 1 demonstrates FTIR spectra of loaded CLDH10, CLDH21 and CLDH22 with chromate. The appearance of ν_3 mode of chromate at 885 cm^{-1} in the FTIR spectra of CLDHsL confirms the intercalation of chromate onto CLDHs which is consistent with what found in the literature [33].

3.1.2. S_{BET}

The nitrogen adsorption/desorption isotherms for the LDH22 and CLDH22 adsorbents were previously investigated [32]. The shape of the adsorption-desorption isotherms is classified as type II with a contribution of type IV using the Brunauer-Deming-Deming-Teller (BDDT) method (according to IUPAC classification). Type II adsorption isotherms are characteristic of macro and non-porous materials whereas the most characteristic feature of the type IV isotherms is the hysteresis loop that is corresponding to the pore condensation occurrence. Hence, a contribution caused by the presence of mesoporous (2–50 nm in size)

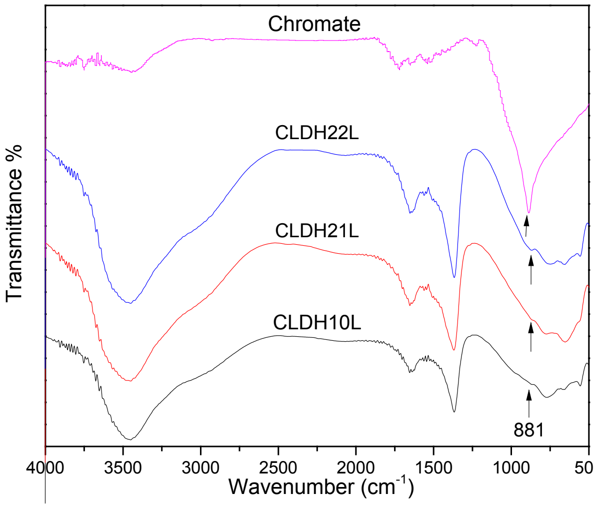

Fig. 1. FTIR spectra of loaded CLDHs with chromate (c).

was concluded from the shape of the isotherm and the presence of a hysteresis loop. Also, the average pore diameter for LDH22 and CLDH22 were 20.9 and 10.2 nm, respectively, that confirmed the meso-porosity of the sorbents. Additionally, the surface area of LDH22 and CLDH22 were estimated to be 70.1 and 198 m^2/g, respectively.

3.1.3. SEM-EDX

Fig. 2 represents SEM micrographs of LDH22, CLDH22 before and after loading with chromate. The characteristic layered texture and the hexagonal crystals of the LDH phase can be seen in Fig. 2a. An obvious disorder and loss of size and crystallinity were observed in the SEM micrograph of CLDH22 (Fig. 2b) owing to the burst loss of CO$_2$ during calcination which was accompanied with an increase in the sorbent surface area [32].

Also, Fig. 2c shows a regain of the ordered hexagonal structure in case of CLDH22L which indicates that the intercalation of chromate into CLDHs is accompanied with the return of the LDH structure which is known as memory effect [35].

Fig. 3 represents the EDX elemental analysis of the CLDH22 (a) and its loaded form CLDH22L (b). Close concentrations of the elements constituting CLDH22 were recorded compared with the bulk elemental analysis (Table 1). The EDX measurements of CLDH22L (3b) indicated the replacement of CrO$_4$ with Cl$^-$ and CO$_3^{2-}$ as concluded from their obvious decrease in concentration or even absence.

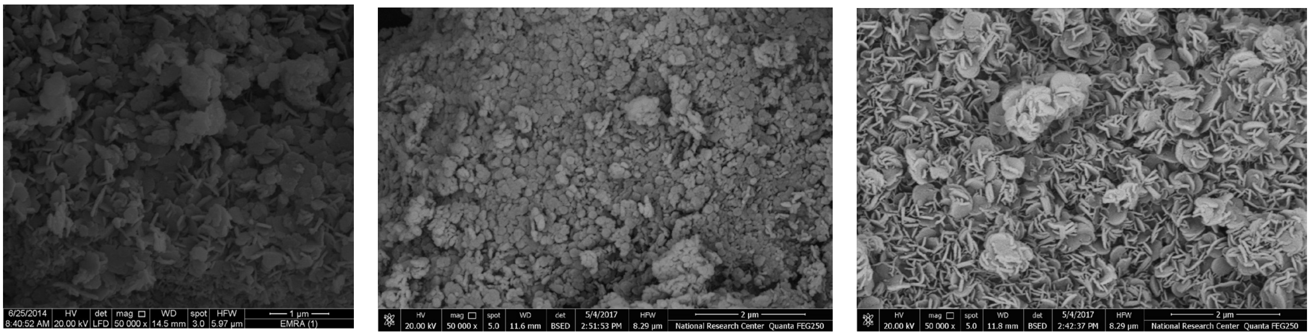

(a) (b) (c)

Fig. 2. SEM micrograph of LDH22 (a), CLDH22 (b) and CLDH22L

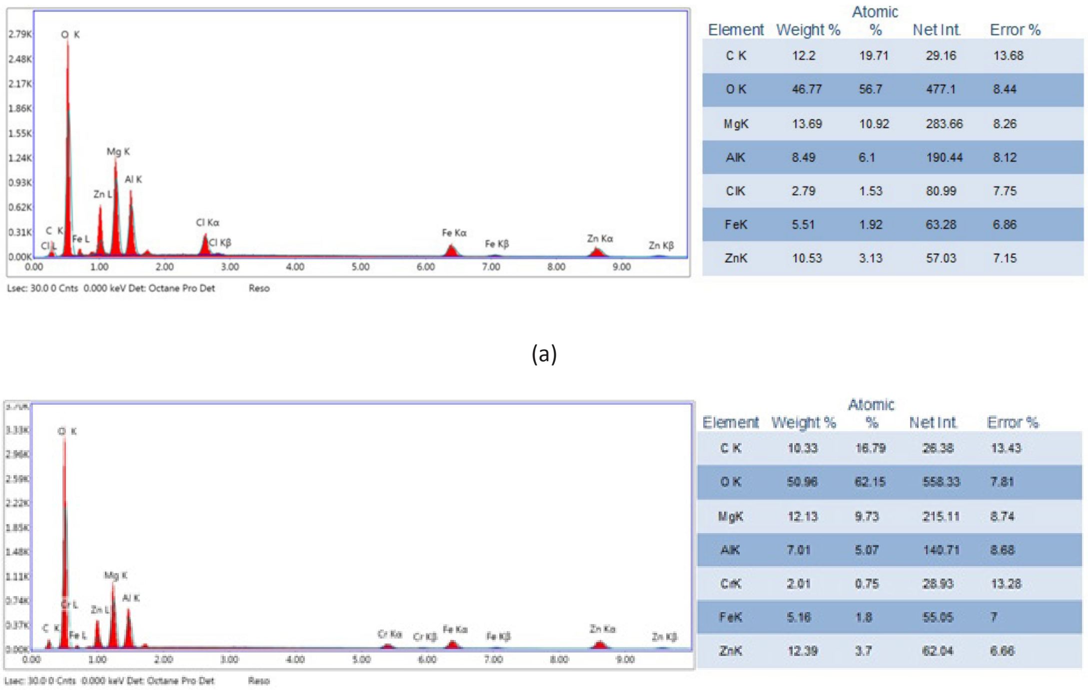

Element	Weight %	Atomic %	Net Int.	Error %
C K	12.2	19.71	29.16	13.68
O K	46.77	56.7	477.1	8.44
MgK	13.69	10.92	283.66	8.26
AlK	8.49	6.1	190.44	8.12
ClK	2.79	1.53	80.99	7.75
FeK	5.51	1.92	63.28	6.86
ZnK	10.53	3.13	57.03	7.15

(a)

Element	Weight %	Atomic %	Net Int.	Error %
C K	10.33	16.79	26.38	13.43
O K	50.96	62.15	558.33	7.81
MgK	12.13	9.73	215.11	8.74
AlK	7.01	5.07	140.71	8.68
CrK	2.01	0.75	28.93	13.28
FeK	5.16	1.8	55.05	7
ZnK	12.39	3.7	62.04	6.66

(b)

Fig. 3. EDX results of CLDH22 (a) and CLDH22L (b).

3.2. Optimization of sorption parameters

3.2.1. Effect of initial pH

Fig. 4 shows the effect of initial pH on sorption capacity of chromate onto CLDHs. At lower pH values (<4), CLDHs sorbents were unstable owing to a partial dissolution occurring in acidic medium. Also, a decrease in sorption capacities was observed for all investigated sorbents at high pH (>8) that may be attributed to the competitive sorption of OH^- ions on CLDHs as a result of increasing pH value. Consequently, the available sites for chromate decreases on the sorbents [36].

The sorbents CLDH10, CLDH21 and CLDH22 have maximum sorption capacities of 27.5, 27.4 and 29.5 mg g^{-1}, respectively, at initial pH of 7.1, which was chosen as an optimum pH value for next studies. The presence of sorption maxima at pH 7.1 may indicate the preferred hosting of CrO_4^{2-} as it is the Cr(VI) ionic species that predominates at a neutral pH range in dilute solutions among other Cr(VI) species [36]. It is important to mention that, the final pH values for all sorbents at all initial pH values rose to 10.08–11.31 as a result of the basic characteristics of CLDHs which may be explained as follows [28]:

$$CLDH\text{-}Cl^- + H_2O + CO_3^{2-} \rightleftharpoons LDH\text{-}CO_3^{2-},Cl^-,OH^- \quad (4)$$

$$LDH\text{-}CO_3^{2-},Cl^-,OH^- + CrO_4^{2-} \rightleftharpoons LDH\text{-}(CrO_4)^- + CO_3^{2-} + Cl^- + OH^- \quad (5)$$

Fig. 5 demonstrates the point of zero charge of CLDHs sorbent. The pH_{PZC} of CLDH10, CLDH21 and CLDH22 was found to be 9.3, 10.2 and 10.4, respectively. This shows that, the CLDHs surface charge was positive at pH less than their pH_{PZC} and negatively charged at solution pH higher than pH_{PZC} [36]. Apparently, the isostructural replacement of Al with Fe raises the stability of the LDH structure which is in accordance with reported results [37]. These characteristics are favorable for the anion exchange property of these sorbents at their optimum pH value (7.1), especially for CLDH22.

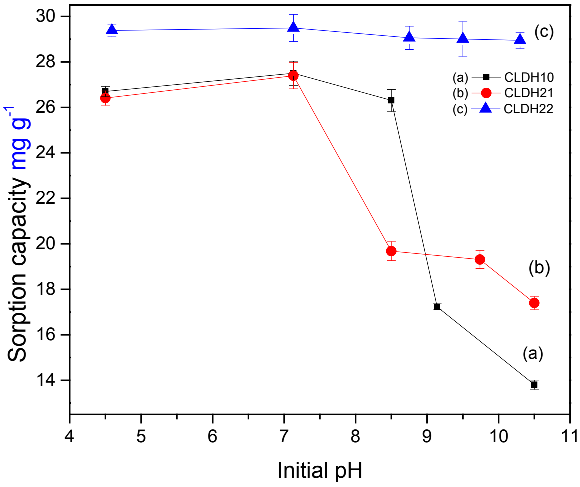

Fig. 4. Effect of initial pH on sorption capacity of chromate onto CLDHs.

3.2.2. Effect of shaking time

Fig. 6 presents the effect of shaking time on sorption capacity of chromate onto CLDHs sorbent. It was observed that, the values of the sorption capacity of chromate by different sorbents proceed rapidly at first, but reached saturation as time progressed. In case of CLDH22, all the sorbate content for the initial concentration 15 mg L^{-1} was sorbed therefore the concentration of 25 mg L^{-1} was applied to enable accurate calculations. This is largely owing to the large abundance of active sites on the sorbents being available at the start of the sorption process [38].

The major part of sorption occurred within the first 30 minutes, where the concentration was almost halved. The rate of sorption of chromate was slow after 3 h, at which 14.4, 14.6 and 24.6 mg g^{-1} of chromate was sorbed onto CLDH10, CLDH21 and CLDH22, respectively.

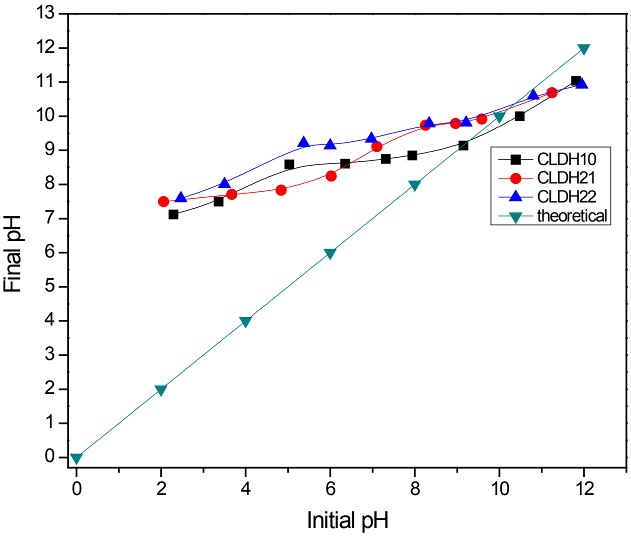

Fig. 5. The point of zero charge (pH_{PZC}) of CLDH.

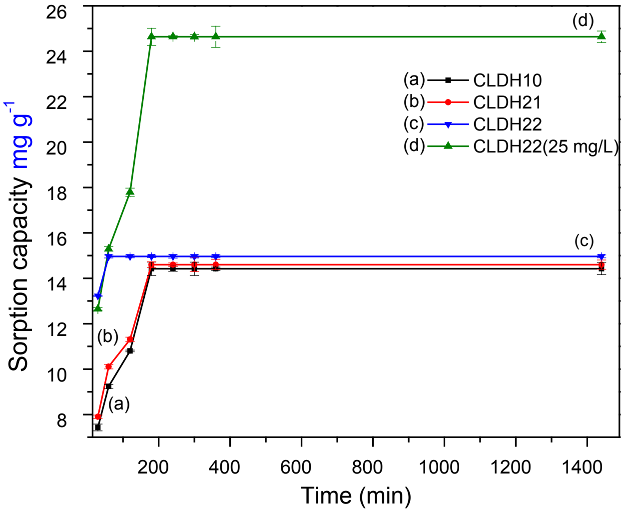

Fig. 6. Effect of shaking time on sorption capacity of chromate onto CLDHs.

3.2.3. Examination of kinetic models

The obtained results of kinetic models fitting are shown in (S7–S10) and Table 3. These results show the good agreement between the experimental and calculated equilibrium sorption q_e for the pseudo 2nd order model confirms that this can better describe correctly the sorption kinetics, based on the high value of $R^2 \geq 0.999$. This behavior was independent of the experimental variables, i.e. sorbent, initial concentration and pH [36]. This supposes that, the heterogeneous chemisorption mechanism is likely to be responsible for the uptake of chromate ions.

3.2.4. Effect of sorbent dose

Fig. 7 illustrates the effect of sorbent dose on sorption capacity of chromate onto the studied CLDHs. It followed the predicted pattern of increasing sorption capacity as dosage increases and reached complete sorption of chromate (>99%) from aqueous solution. This is due to the fact that as the sorbent dose increases, the surface area available increases and larger number of sorption sites is available to sorb chromate with enhanced uptake [39].

Complete removal of 50 mg L^{-1} of chromate (>99%) was achieved at sorbent dose ≥ 50 mg (0.2% w/v) of CLDHs and (>92%) was achieved at 25 mg (0.1% w/v) of CLDH22. The observed low dosage of CLDH22 required to achieve complete removal of chromate ion is an important advantage from the economical aspect.

3.2.5. Effect of initial concentration

Fig. 8 represents the effect of initial concentration on the removal efficiency of chromate onto the studied CLDHs. The low uptake at higher concentration resulted from an increased ratio of initial number of moles of chromate to the available surface area; hence fractional sorption becomes dependent on initial concentration. For a given sorbent dose, the total number of available sorption sites is fixed, thereby sorbing almost the same amount of sorbate. Thus, this results in decreasing in the removal of sorbate concentration (saturation of sorbent) due to competition of chromate molecules for the active sorption sites of sorbents [40].

The removal efficiencies of chromate ions observed to decrease in the range of (96.14–86.06 (a), 97.34–85.60 (b) and 99.52–91.18 (c))% using CLDH10, CLDH21 and CLDH22, respectively, as sorbents.

3.2.6. Fitting of sorption isotherm models

The sorption isotherm models; Langmuir, Freundlich and Redlich-Peterson (S11–S13) were examined for chromate sorption onto CLDHs and their resulting parameters are listed in Table (4).The dimensionless equilibrium factors (R_L) were found less than 1 and greater than zero, ($0 < R_L < 1$), indicating a favorable sorption process. The n values

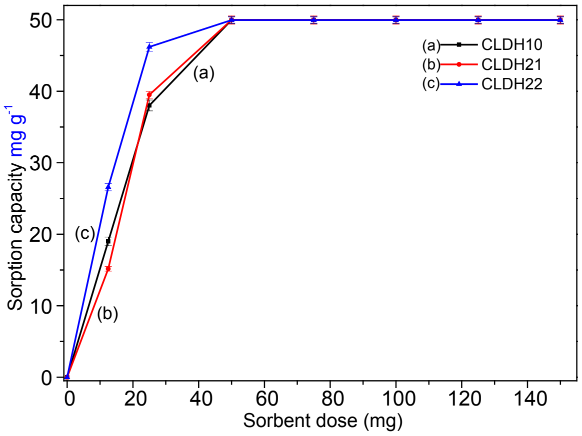

Fig. 7. Effect of sorbent dose on sorption capacity of chromate anion onto CLDHs.

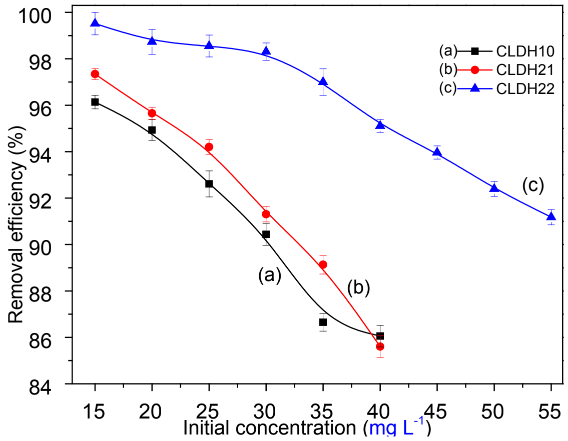

Fig. 8. Effect of initial concentration on removal efficiency of chromate anion onto CLDHs.

Table 3
Kinetic model constants and correlation coefficients for chromate sorption onto CLDHs sorbent, $C_i = 15$ mg L^{-1}

Sorbent	q_e,(exp) (mg g^{-1})	Pseudo-first order			Pseudo-second order			Intraparticle diffusion rate		Liquid film diffusion	
		k_1 (min^{-1})	q_e,(cal) (mg g^{-1})	R^2	k_2 (g $mg^{-1}min^{-1}$)	$q_{e,\ cal}$ (mg g^{-1})	R^2	K_p (g mg^{-1} $h^{0.5}$)	R^2	R^1	R^2
CLDH10	14.42	0.013	3.673	0.517	0.002	14.71	0.999	0.199	0.568	0.003	0.527
CLDH21	14.60	0.011	2.974	0.522	0.003	14.93	0.999	0.181	0.514	0.003	0.513
CLDH22	14.96	0.010	6.801	0.517	0.086	14.98	0.999	0.348	0.599	0.004	0.537

Table 4
Langmuir, Freundlich and Redlich-Peterson's parameters for chromate onto CLDHs

Sorbent	q_{max}(exp) $mg\ g^{-1}$	Langmuir parameters				Freundlich parameters			Redlich-Peterson		
		q_{max}(cal) $mg\ g^{-1}$	R_L	b_L $L\ mg^{-1}$	R^2	K_F	n	R^2	g	a_R (L/mg)	R^2
CLDH10	34.42	40.0	0.028–0.072	0.862	0.986	18.38	2.747	0.973	0.978	1.101	0.993
CLDH21	34.24	38.46	0.021–0.053	1.182	0.993	20.07	3.106	0.992	0.947	1.970	0.992
CLDH22	50.15	52.63	0.008–0.027	2.375	0.987	32.14	3.484	0.979	0.997	6.107	0.959

are in the range from (2.7–3.5) that represent a good sorption potential of the sorbent, which indicates a good energy distribution on the sorbent surface [41]. The g exponential values are less than 1.

The experimental data indicate that the sorptive behaviors of chromate onto CLDHs could be better represented by the Langmuir's isotherm as its coefficient of determination, R^2 were 0.986–0.993 the highest. This also demonstrates that, chromate is sorbed onto sorbents as monolayer sorption.

This refers to that; chromate could be easily sorbed on the different CLDH sorbents. Therefore, the theoretical maximum sorption capacity, q_{cal} evaluated from Langmuir's model was found to be 40.0, 38.5 and 52.6 mg $g^{-1} \equiv$ 34.8, 33.5 and 45.7 mmol/100 g for CLDH10, CLDH21 and CLDH22, respectively, which are close to the experimental values, $q_{max\text{-}(exp)}$ 34.4, 34.2 and 50.2 mg g^{-1}, respectively. Accordingly, CLDH22 was considered as the optimal structure for the sorption of Cr(VI) attributed to the appropriate Zn(II) and Fe(III) ratios inserted into the Mg/Al-LDH structure [37,42].

3.2.7 Effect of temperature

Effect of temperature on sorption capacity of chromate onto CLDH22 as a representative for the studied CLDHs is presented in Fig. 9. It was found that, the sorption capacity increases with increasing the temperature until 40°C. The enhanced removal of chromate ions onto CLDH22 sorbent may be attributed to the increase of mobility of chromate ions, the swelling of pore structure of the sorbent and decrease the retarding forces between the sorbate ions and sorbent [39].

3.2.8 Determination of the thermodynamic parameters

The thermodynamic parameters of sorption of chromate on CLDH22, as an example, were calculated and the data are listed in Table 5.

The values of ΔG_{ads} are negative, confirming that the sorption of chromate ions on CLDH22 is a spontaneous and thermodynamically favorable. The more negative values of ΔG_{ads} imply a greater driving force to the sorption process.

The value of ΔH_{ads} is positive, indicating that the sorption process is endothermic in nature. The value of ΔH_{ads} is moderately high ensuring an adequate interaction between the chromate ions and CLDH22. Generally, the value of ΔH_{ads} for the physical sorption is <20.0 KJ mol^{-1}, while that of chemisorption is in the range 80–200 KJ mol^{-1} [43]. The obtained value of ΔH_{ads} for this case is indicating that the process is controlled by a spontaneous mixed physico- and chemisorption processes which is in agreement with the suggested intercalation mechanism of chromate ions in the Van der Waal's gap [23].

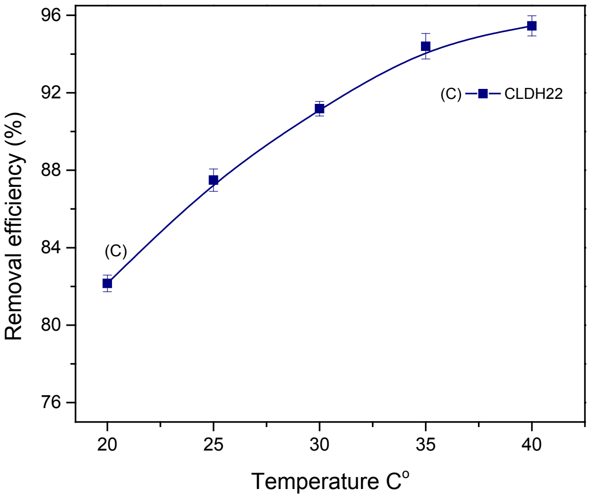

Fig. 9. Effect of temperature on removal efficiency of chromate anion onto CLDH22.

Table 5
The thermodynamic parameters of chromate sorption onto CLDH22, $C_i = 55$ mg L^{-1}

T (K)	ΔH_{ads} (kJ mol^{-1})	ΔS_{ads} (kJ K^{-1} mol^{-1})	$-\Delta G_{ads}$ (kJ mol^{-1})	R^2
293	59.79	0.217	3.747	0.989
298			4.832	
303			5.916	
308			7.0	
313			8.084	

The positive value of ΔS may be attributed to the increase in randomness during the intercalation of chromate ions on CLDH22. The increase in randomness also arises from the recovery of LDH structure in the so-called 'memory effect' when contacted with chromate solution. This was confirmed by the recovery of the layered structure (Fig. 2c) and the detection of Cr (Fig. 3b) in the loaded sample according to SEM-EDX measure. These results infer that the endothermic sorption is entropically driven.

It is noteworthy to mention that, the Fe-containing CLDHs (CLDH22 and CLDH21) showed good magnetic properties that it could be easily collected by a magnet after loading with chromate as illustrated in Fig. 10 as an example.

3.3. Desorption study

Table 6 shows desorption results of chromate-loaded onto CLDHs using different eluents (NaCl, NaOH or Na_2CO_3) with concentrations 0.1 or 1.0 mol L^{-1}, at 30°C. The order of elution efficiency of chromate from CLDHs was Na_2CO_3 > NaOH > NaCl, which indicates the relative intercalation preferences of their anions. This was attributed to the high degree of affinity of carbonate for LDH [39,44].

Usage of 1.0 mol L^{-1} Na_2CO_3 increased the single-batch elution efficiency of chromate up to 99.74, 94.02 or 53.25% using CLDH10, CLDH21 or CLDH22, respectively. Almost quantitative desorption of chromate for CLDH10 and CLDH21 and incomplete elution for CLDH22 indicates the relative hosting preference of chromate onto CLDH22. However, repeated desorption processes should enable complete recovery of chromate that assures the formation of no secondary waste materials during application and ability of reusing sorbents.

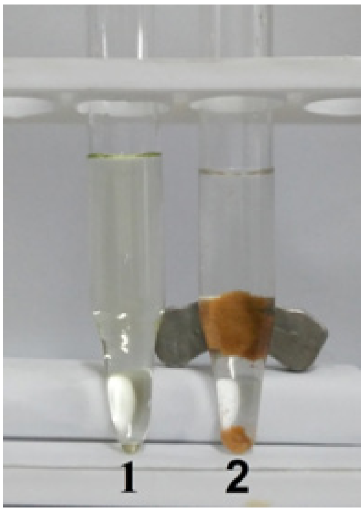

Fig. 10. Magnetic separation of loaded chromate onto CLDH22 ('1', C_i = 55 mg L^{-1} and '2', C_f = 4.9 mg L^{-1}).

Table 6
Desorption study of chromate-loaded onto CLDHs at 30°C

Eluent	Concentration of eluent, mol L^{-1}	Eluted chromate (%) at 30°C		
		CLDH10	CLDH21	CLDH22
NaCl	0.1	14.07	19.02	0.504
NaOH	0.1	39.25	41.03	12.99
Na_2CO_3	0.1	85.94	79.62	39.75
Na_2CO_3	1.0	99.74	94.02	53.25

3.4. Removal of Cr at optimized conditions

3.4.1. Removal of Cr(III) after preliminary oxidation

The removal process of Cr(VI) onto the most efficient sorbent; CLDH22, was aimed to be developed to include Cr(III) as well, due to the common presence of both species in waste and contaminated samples. To emphasize this goal the removal process was examined on standard solution of Cr(III) (50 mg L^{-1}) in 25 mL after preliminary oxidation with H_2O_2 in a basic medium. Table 7 lists the removal efficiencies of total Cr(III and VI) onto CLDH22 sorbent. The obtained removal efficiency was 94.31%, which is comparable to pure Cr(VI) removal results. Comparing the present removal efficiency of CLDH for Cr(III) with newly reported fluorinated activated BN (F-ABN) sorbent (82.6%) [23], it may be recognized that CLDH has a higher sorption capacity, faster kinetics and lesser minimum dosage for Cr(III) removal.

3.4.2. Removal of total Cr(III and VI) from contaminated samples

The removal process was applied on a stock of 50 mg L^{-1} Cr(III) prepared from standard reference material, waste and contaminated samples with CLDH22 to remove Cr(VI) or Cr(III+VI) either directly or after oxidation.

The removal of Cr(VI) for all studied samples was appreciably high in the range 98.4100% due to their low Cr(VI) content. Also, good removal efficiencies were obtained for Cr(III) (after oxidation) 88.5–92.7% as detailed in Table 7. The successful removal of Cr(VI) and Cr(III) from contaminated samples of different origins and backgrounds confirms the potential validity of CLDH22 as removal sorbent for these ions.

Comparisons between uptake capacities of CLDH22, different recent CLDHs and common sorbents towards chromate anion are presented in Table 8. From these com-

Table 7
The removal of total Cr(III and VI) onto CLDH22

Sample	Total Cr, mg mL^{-1}	Cr(VI), µg mL^{-1}	Cr(III), mg mL^{-1}	R of Cr(VI),%	R of Cr(III + VI) after oxidation, %
A stock 50 mg mL^{-1} prepared from standard reference material of Cr	49.74	–	49.74	–	94.31
Tanning effluent (A)	2.61	11.5	2.60	99.6	88.5
Tanning effluent (B)	13.6	29.1	13.5	98.4	90.7
Tanned leather scraps (extract)	24.6	771	23.8	99.4	92.7
White cement* suspension	1.23*	1.23*	–	100	–
Portland cement* suspension	6.41*	6.41*	–	99.9	–

*Cr concentrations in cement samples are given in ppm unit

Table 8
Uptake capacities of CLDH22, recent CLDHs and common sorbents towards chromium(VI)

Sorbent	Metal molar ratios (starting salt)	A^-	Calcination temperature, °C	Equilibrium time, h	Removal capacity[c], mmol/100 g[c]	Ref.
CLDH	Mg/Al 1.4:1 (nitrates)	CO_3^{2-}	350	24	32.6	[45]
CLDH	Zn/Al 1:1 (nitrates)	CO_3^{2-}	500	1	10.9	[23]
CLDH	Fe_3O_4-Zn/Al 2.37:1 (nitrates)	CO_3^{2-}	500	1	9.95	[23]
CLDH	Mg/Al-Fe 6:1 (nitrates)	CO_3^{2-}/NO_3^-	450	24	16.2	[46]
CLDH	Mg/Al 3.47:1 (chlorides)	CO_3^{2-}/Cl^-	450	6	10.5	[32]
CLDH	Mg/Zn/Al/Fe 2.76:0.19:0.87:0.13 (chlorides)	CO_3^{2-}/Cl^-	450	6	27.9	[32]
CLDH	Graphene-Mg/Al (nitrates)	CO_3^{2-}	500	–	3.72	[28]
CLDH	Ni/Mg/Al/urea 1:1:1:6 (Sulfates+nitrate)	-	600	2.5	53.5	[20]
LDHs@MoS2	Mg/Al/Mo/S2 6.7:2.2:0.68:1.3 (chlorides)	CO_3^{2-}	200	24	35.3	[47]
Ni/Mg/Al-LDO	Ni/Mg/Al 1:1:1:6 (Sulfates+nitrate)	-	600	5	47.9	[48]
Titanium dioxide coated carbon sphere	C@La-TiO_2	-	200	4	23.4	[49]
Magnetic porous carbonaceous	MPC-300	-	300	3	9.83	[50]
Organoclays C12mim Br-Mt C16mim Br-Mt	C12mim Br C16mim Br	-	-	2	9.70 11.4	[51]
Fe_3O_4-polyethyleneimine-steam exploded rice straw	Fe_3O_4-PEI-SERS	-	45[h]	6	129	[52]
Sewage sludge compost biomass	-	-	-	48	1.63	[53]
Thermally sodium organo-bentonite biopolymer composite	TSOBC	-	-	3	57.5	[54]
The magnetic iron oxide nanoparticles	MIONPs	-	-	1	16.0	[55]
Hyperbranched polyamide modified corncob	HPMC	-	70[h]	4	60.9	[56]
carboxylated cellulose nanocrystals polyethyleneimine	CCN-PEI	-	60	10	166	[57]
Nitrogen-doped magnetic biochar $FeCl_3$	ABF-N800		800	7	66.1	[58]
Corn stalk fibers	CSF	-	80	10 min	67.1	[60]
CLDH22	Mg/Zn/Al/Fe 2.30:0.56:0.74:0.26 (chlorides)	CO_3^{2-}/Cl^-	450	3	45.7[a]	Present work

[a] Removal capacity (mmol/100 g) for CLDH22 was estimated according to mathematical relationship,

$$Capacity\left(mmol/100\,g\right)=\frac{q_{\max,cal}\left(\frac{mg}{g}\right)}{M\left(\frac{g}{mol}\right)}\times 100$$

where $q_{max,cal}$ is the maximum sorption capacity of chromate onto CLDH22, and M is the molecular weight of chromate.

[c] denotes 'calculated from the publication' to ease comparison; [h] denotes hydrothermally aged.

parisons, CLH22 is apparently characterized by higher capacity and faster kinetics of chromate sorption.

4. Conclusion

The newly reported calcined layered double hydroxide denoted CLDH10, CLDH21 and CLDH22 sorbents were evaluated as potential sorbent for Cr(VI) from wastewater and contaminated samples. Chromate was optimally extracted at pH 7.1 after 3 h of shaking. The complete removal (>99%) of chromate was achieved at sorbent dosage ≥50 mg (0.2% w/v) of the investigated CLDHs. Also, (>92%) of chromate can be removed using CLDH22 even at lower dose (1 g L^{-1}). The sorption process was found to follow the pseudo-second order kinetics and Langmuir-type isotherm with monolayer capacities 40.0, 38.5 and 52.6 mg g^{-1}, onto CLDH10, CLDH21 and CLDH22 sorbents, respectively. The measured thermodynamic parameters ΔG_{ads}, ΔH_{ads} and ΔS_{ads} indicated that the intercalation process of chromate onto CLDH22 was spontaneous and endothermic in nature. FTIR, SEM, EDXand FAAS confirmed the loading of Cr(VI). The magnetic separation of chromate anions onto Fe-containing sorbents were demonstrated which may facilitate the separation process on real application. One molar Na_2CO_3 was considered the most efficient eluent for loaded chromate from CLDH sorbents. CLDH22 sorbent was evidenced as a potential sorbent for the removal of Cr(VI) and Cr(III) (after preliminary oxidation) from standard reference material, tanning effluents, leather scraps and cement extracts with removal efficiencies from 88.5–100%.

Dedication

It is our genuine gratefulness and warmest regard that we dedicate this work to the sole of *Prof. Dr/ Medhat A. H. Hafez* for his devotion and guidance.

Acknowledgement

The authors deeply thank Prof. Dr. Elshahat Nashy, Chemistry of Tanning Materials and Leather Technology Department, National Research Centre, Dokki, Giza, Egypt, for advice and cooperation. Also, the authors wish to express their gratitude to Dr. D. Schiel, PTB-Braunschweig, Braunschweig, Germany for supplying the Cr reference sample.

References

[1] D.M. Whitacre, Reviews of Environmental Contamination and Toxicology, vol. 232, Springer, New York, 2014.

[2] C. Bourotte, R. Bertolo, M. Almodovar, R. Hirata, Natural occurrence of hexavalent chromium in a sedimentary aquifer in Urânia, State of São Paulo, Brazil, An. Acad. Braz. Sci., 81 (2009) 227–242.

[3] R.K. Gautam, S.K. Sharma, S. Mahiya, M.C. Chattopadhyaya, Chapter 1: Contamination of Heavy Metals in Aquatic Media: Transport, Toxicity and Technologies for Remediation, in Heavy Metals In Water: Presence, Removal and Safety, 2014, pp. 1–24.

[4] H-L. Huang, H-H. Huang, Y.J. Wei, Reduction of toxic Cr(VI)-humic acid in an ionic liquid, Spectrochim. Acta B, 133 (2017) 9–13.

[5] A. Zhitkovich, Chromium in drinking water: sources, metabolism, and cancer risks, Chem. Res. Toxicol., 24 (2011) 1617–1629.

[6] A.D. Dayan, A.J. Paine, Mechanisms of chromium toxicity, carcinogenicity and allergenicity: review of the literature from 1985 to 2000, Hum. Exp. Toxicol., 20 (2001) 439–451.

[7] A.S. Dharnaik, P.K. Ghosh, Hexavalent chromium [Cr(VI)] removal by the electrochemical ion-exchange process, Environ. Tech., 35 (2014) 2272–2279.

[8] A.A. Lewinsky, Hazardous Materials and Wastewater: Treatment, Removal and Analysis, New York : Nova Science Publishers, Inc., 2007.

[9] T. Ahmad, M. Danish, M. Rafatullah, A. Ghazali, O. Sulaiman, R. Hashim, M. Ibrahim, The use of date palm as a potential adsorbent for wastewater treatment: a review, Environ. Sci. Pollut. Res. 19 (2012) 1464–1484.

[10] H. Thatoi, S. Das, J. Mishra, B.P. Rath, N. Das, Bacterial chromate reductase, a potential enzyme for bioremediation of hexavalent chromium: a review, J. Environ. Manage., 146 (2014) 383–399.

[11] S. Hokkanen, E. Repo, M. Sillanpää, Removal of heavy metals from aqueous solutions by succinic anhydride modified mercerized nanocellulose, Chem. Eng. J., 223 (2013) 40–47.

[12] G.M. Nabil, N.M. El-Mallah, M.E. Mahmoud, Enhanced decolorization of reactive black 5 dye by active carbon sorbent-immobilized-cationic surfactant (AC-CS), Ind. Eng. Chem., 20 (2014) 994–1002.

[13] D. Kang, X. Yu, S. Tong, M. Ge, J. Zuo, C. Cao, W. Song, Performance and mechanism of Mg/Fe layered double hydroxides for fluoride and arsenate removal from aqueous solution, Chem. Eng. J., 228 (2013) 731–740.

[14] S. Miyata, Anion exchange properties of hydrotalcite-like compounds, Clays Clay Miner., 31 (1983) 305–311.

[15] F. Cavani, F. Trifirò, A. Vaccari, Hydrotalcite-type anionic clays: preparation, properties and applications, Catal. Today, 11(2) (1991) 173–301.

[16] P. Gu, S. Zhang, X. Li, X. Wang, T. Wen, R. Jehan, A. Alsaedi, T. Hayat, X. Wang, Recent advances in layered double hydroxide-based nanomaterials for the removal of radionuclides from aqueous solution, Environ. Pollut., 240 (2018) 493e505.

[17] S.M. Auerbach, K.A. Carrado, P.K. Dutta, Handbook of Layered Materials, New York, NY: Marcel Dekker, 2004, pp. 377.

[18] S. Radha, A. Navrotsky, Energetics of CO_2 adsorption on Mg–Al layered double hHydroxides and related mixed metal oxides, J. Phys. Chem., 118 (2014) 29836–29844.

[19] M. Sajid, C. Basheer, Layered double hydroxides: Emerging sorbent materials for analytical extractions, Trends Anal. Chem., 75 (2016) 174–182.

[20] C. Lei, X. Zhu, B. Zhu, C. Jiang, Y. Le, J. Yu, Superb adsorption capacity of hierarchical calcined Ni/Mg/Al layered double hydroxides for Congo red and Cr(VI) ions, J. Hazard. Mater., 321 (2017) 801–811.

[21] L. Zhong, X. He, J. Qu, X. Li, Z. Lei, Q. Zhang, X. Liu, Precursor preparation for Ca-Al layered double hydroxide to remove hexavalent chromium coexisting with calcium and magnesium chlorides, J. Solid State Chem., 245 (2017) 200–206.

[22] A. Jaiswal, R. Mani, S. Banerjee, R.K. Gautam, M.C. Chattopadhyaya, Synthesis of novel nano-layered double hydroxide by urea hydrolysis method and their application in removal of chromium(VI) from aqueous solution: Kinetic, thermodynamic and equilibrium studies, J. Mol. Liq., 202 (2015) 52–61.

[23] L-g. Yan, K. Yang, R-r. Shan, H-q. Yu, B. Du, Calcined ZnAl- and Fe_3O_4/ZnAl–layered double hydroxides for efficient removal of Cr(VI) from aqueous solution, RSC Adv., 5 (2015) 96495.

[24] B. Hu, W. Liu, W. Gao, J. Han, H. Liu, L.A. Lucia, Pseudo-Janus Zn/Al-based nanocomposites for Cr(VI) sorption/remediation and evolved photocatalytic functionality, Chem. Eng. J., 277 (2015) 150–158.

[25] G. Eshaq, A.M. Rabie, A.A. Bakr, A.H. Mady, A.E. ElMetwally, Cr(VI) adsorption from aqueous solutions onto Mg–Zn–Al LDH and its corresponding oxide, Desal. Water Treat., 57(43) (2016) 20377–20387

[26] W. Wang, J. Zhou, G. Achari, J. Yu, W. Cai, Cr(VI) removal from aqueous solutions by hydrothermal synthetic layered double hydroxides: Adsorption performance, coexisting anions and regeneration studies, Colloids Surf. A: Physicochem. Eng. Asp., 457 (2014) 33–40.

[27] M. Khitous, Z. Salem, D. Halliche, Effect of interlayer anions on chromium removal using Mg–Al layered double hydroxides: Kinetic, equilibrium and thermodynamic studies, Chinese J. Chem. Eng., 24 (2016) 433–445.

[28] X. Yuan, Y. Wang, J. Wang, C. Zhou, Q. Tang, X. Rao, Calcined graphene/MgAl-layered double hydroxides for enhanced Cr(VI) removal, Chem. Eng. J., 221 (2013) 204–213.

[29] Y. Zou, X. Wang, A. Khan, P. Wang, Y. Liu, A. Alsaedi, T. Hayat, X. Wang, Environmental remediation and application of nanoscale zero-valent iron and its composites for the removal of heavy metal ions: a review, Environ. Sci. Technol., 50 (2016) 7290–7304.

[30] J. Li, X. Wang, G. Zhao, C. Chen, Z. Chai, A. Alsaedi, T. Hayat, X. Wang, Metal–organic framework-based materials: superior adsorbents for the capture of toxic and radioactive metal ions, Chem. Soc. Rev., 47 (2018) 2322–2356.

[31] G. Zhao, X. Huang, Z. Tang, Q. Huang, F. Niu, X. Wang, Polymer-based nanocomposites for heavy metal ions removal from aqueous solution: a review, Polym. Chem., 9 (2018) 3562–3582.

[32] K.S. Abou-El-Sherbini, I.M.M. Kenawy, M.A.H. Hafez, H.R. Lotfy, Z.M. Abd Elbary, Synthesis of novel CO_3^{2-}/Cl^- bearing 3(Mg+Zn)/(Al +Fe) layered double hydroxides for the removal of anionic hazards, JECE, 3 (2015) 2707–2721.

[33] J. Mendham, R.C. Denney, J.D. Barnes, M. Thomas, B. Sivasankar, Quantitative chemical analysis, 6th ed., Vogel's textbook, Pearson Education Ltd., New Delhi, India, 2000, pp. 58, 311–335, 349, 651, 70, 340.

[34] Z. Marczenko, Separation and spectrophotometeric determination of elements"; Ellis Horwood Limited, New York, 2nd ed., 1986, pp. 21–43,134.

[35] D.G. Evans, R.C.T. Slade, Layered double hydroxides, Struct. Bond., 119 (2006) 6.

[36] A. Elhalil, S. Qourzal, F.Z. Mahjoubi, R. Elmoubarki, M. Farnane, H. Tounsadi, M. Sadiqa, M. Abdennouri, N. Barka, Defluoridation of groundwater by calcined Mg/Al layered double hydroxide, Emerg. Contam., 2 (2016) 42–48.

[37] K.B. Rozov, U. Berner, D.A. Kulik, L.W. Diamond, Solubility and thermodynamic properties of carbonate-bearing hydrotalcite-pyroaurite solid solutions with a 3:1 Mg/(Al+Fe)mole ratio, Clays Clay Miner., 59 (2011) 215–232.

[38] J.T. Kloprogge (ed), The Application of Vibrational Spectroscopy to Clay Minerals and Layered Double Hydroxides, Clay Minerals Society, Aurora, 2005.

[39] K-H. Goh, T-T. Lim, Z. Dong, Application of layered double hydroxides for removal of oxyanions: A review, Water Res., 42 (2008) 1343–1368.

[40] N.Y. Mezenner, A. Bensmaili, Kinetics and thermodynamic study of phosphate sorption on iron hydroxide-eggshell waste, Chem. Eng. J., 147 (2009) 87–96.

[41] K.Y. Foo, B.H. Hameed, Insights into the modeling of adsorption isotherm systems, Chem. Eng. J., 156 (2010) 2–10.

[42] P.-P. Huang, C.-Y. Cao, F. Wei, Y.-B. Sun, W.-G. Song, MgAl layered double hydroxides with chloride and carbonate ions as interlayer anions for removal of arsenic and fluoride ions in water, RSC Adv., 5 (2015) 10412–10417.

[43] Y. Liu, Y.-J. Liu, Biosorption isotherms, kinetics and thermodynamics, Sep. Purif. Technol., 61 (2008) 229–242.

[44] J. Flores, E. Lima, M. Maubert, E. Aduna, J.L. Rivera, Clean-up of wastes from the textile industry using anionic clays, Clays Clay Min., 59 (2011) 240–249.

[45] X. Song, Y. Wu, Simultaneous sorption of chromium (VI) and phosphate by calcined Mg-Al-CO_3layered double hydroxides, Bull. Korean Chem. Soc., 35 (2014) 1817–1824.

[46] F. Zhang, N. Du, H. Li, S. Song, W. Hou, Sorbent effect on the sorption of Cr(VI) on a Mg6AlFe-layered double hydroxide and its calcined product in aqueous solutions, Colloid. Polym. Sci., 293 (2015) 1961–1969.

[47] J. Wang, P. Wang, H. Wang, J. Dong, W. Chen, X. Wang, S. Wang, T. Hayat, A. Alsaedi, X. Wang, Preparation of molybdenum disulfide coated mg/al layered double hydroxide composites for efficient removal of chromium(VI), ACS Sustain. Chem. Eng., 5 (2017) 7165–7174.

[48] C. Lei, X. Zhu, B. Zhu, C. Jiang, Y. Le, J. Yu, Superb adsorption capacity of hierarchical calcined Ni/Mg/Al layered double hydroxides for Congo red and Cr(VI) ions, J. Hazard. Mater., 321 (2017) 801–811.

[49] J. Wang, Y. Liang, Q. Jin, J. Hou, B. Liu, X. Li, W. Chen, T. Hayat, A. Ahmed, X. Wan, Simultaneous removal of graphene oxide and chromium(VI) on the rare earth doped titanium dioxide coated carbon sphere composites, ACS Sustain. Chem. Eng., 5 (2017) 5550–5561.

[50] T. Wen, J. Wang, S. Yu, Z. Chen, T. Hayat, X. Wang, Magnetic porous carbonaceous material produced from tea waste for efficient removal of As(V), Cr(VI), humic acid and dyes, ACS Sustain. Chem. Eng., 5 (2017) 4371–4380.

[51] Y. Liang, Y. Li, S. Zhang, H. Li, X. Mao, L. Zhou, W. Yang, Equilibrium, kinetics, and thermodynamics studies of Cr(VI) adsorption from aqueous solutions on organoclay using ionic liquid-type imidazolium surfactants, Desal. Water Treat., 100 (2017) 135–144.

[52] S. Zhang, Z. Wang, H. Chen, C. Kai, M. Jiang, Q. Wang, Z. Zhou, Polyethylenimine functionalized Fe_3O_4/steam-exploded rice straw composite as an efficient adsorbent for Cr(VI) removal, Appl. Surf. Sci., 440 (2018) 1277–1285.

[53] H. Chen, J. Dou, H. Xu, Removal of Cr(VI) ions by sewage sludge compost biomass from aqueous solutions: Reduction to Cr(III) and biosorption, Appl. Surf. Sci., 425 (2017) 728–735.

[54] M.H. Dehghani, A. Zarei, A. Mesdaghin, Adsorption of Cr(VI) ions from aqueous systems using thermally sodium organo-bentonite biopolymer composite (TSOBC): response surface methodology, isotherm, kinetic and thermodynamic studies, Desal. Water Treat., 85 (2017) 298–312.

[55] S. Lin, C. Lian, M. Xu, W. Zhang, L. Liu, K. Lin, Study on competitive adsorption mechanism among oxyacid-type heavy metals in co-existing system: Removal of aqueous As(V), Cr(III) and As(III) using magnetic iron oxide nanoparticles (MIONPs) as adsorbents, Appl. Surf. Sci., 422 (2017) 675–681.

[56] H. Lin, S. Han, Y. Dong, Y. He, The surface characteristics of hyperbranched polyamidemodified corncoband its adsorption property for Cr(VI), Appl. Surf. Sci., 412 (2017) 152–159.

[57] C. Liu, R-N. Jin, X-k. Ouyang, Y-G. Wang, Adsorption behavior of carboxylated cellulose nanocrystal—polyethyleneimine composite for removal of Cr(VI) ions, Appl. Surf. Sci., 408 (2017) 77–87.

[58] Md. Mian, G. Liu, B. Yousaf, B. Fu, H. Ullah, M. Ali, Q. Abbas, M. Munir, L. Ruijia, Simultaneous functionalization and magnetization of biochar via NH_3 ambiance pyrolysis for efficient removal of Cr (VI), Chemosphere, 208 (2018) 712–721.

[60] X. Wen, N. Sun, C. Yan, S. Zhou, T. Pang, Rapid removal of Cr(VI) ions by densely grafted corn stalk fibers: High adsorption capacity and excellent recyclable property, J. Taiwan Inst. Chem. Eng. 000 (2018) 1–10.

Supplementary

S1: Synthesis and analysis of the sorbents

An aqueous solution of Mg(II), Zn(II), Al(III) and Fe(III) chlorides with initial metal ratios of 2.7:0.3:1.0:0, 2.4:0.6:0.9:0.1 and 2.4:0.6:0.8:0.2 was prepared, LDHs were precipitated by the simultaneous dropwise addition of 100 mL of a total of 2.5 mol L^{-1} of the mixture of the metal chlorides to a basic carbonate solution (NaOH, Na_2CO_3). The suspension was adjusted at pH = 10, kept at 70–80°C for a week and subsequently filtered. The resulting precipitate was washed repeatedly for 10 times with bi-distilled water, then dried at 70ºC for 48 h, kept in a desiccator and coded LDH10, LDH21 and LDH22, respectively. Calcined LDH (CLDH) was obtained by thermal treatment of LDH materials at 450ºC for 3 h and coded CLDH10, CLDH21 and CLDH22, respectively. CLDHs were cooled to room temperature and kept in desiccator.

For elemental analysis, appropriate amounts of synthesized LDHs were dissolved in HCl (HNO_3 was used in case of Cl% determination), and diluted to 100 mL. The concentration of Mg^{2+}, Zn^{2+} and Fe^{3+} was determined by complexometric titration with EDTA [1]. Mg^{2+} and Zn^{2+} were titrated at pH = 10 simultaneously using Eriochrome black T (EBT) as indicator, then Zn^{2+}, in another sample, was masked by KCN to determine the concentration of Mg^{2+} alone. Fe^{3+} was titrated in acidic medium (pH = 2) using xylenol orange as indicator. Al^{3+} is spectrometrically determined at 535 nm using Eriochrome cyanine R as indicator at pH = 6–6.2 in the presence of ascorbic acid to avoid the interference of Fe^{3+} [2]. Chloride ion is determined by Mohr's method [1].

S2: Micro-structural and mineralogical characterization

The chemical composition of the contaminated real samples (given in Table 2), was assessed as follows: Electrical conductivity (EC) was measured by using a Jenco 3173 Conductivity/TDS/Temperature benchtop meter, Chatsworth, CA, USA. Na and K concentration was determined using a JENWAY Flame Photometer model PFP7 conductometer from Dibby Scientific Limited, Essex, UK. A Perkin Elmer model 3110 flame atomic absorption spectrometer (FAAS) was used for the determination of total Cr. Sulfate (SO_4) content was analyzed by back titration [3]. Also, Mg and Ca were determined following standard methods [4].

S3

The point zero charge (pH_{PZC}) of CLDH sorbents was determined by the adjustment of initial pH of 0.1 M NaCl solutions to a pH range of 2–12 using 0.01 M HCl or NaOH. Then, 25 mg of the different sorbents was added to each solution. The dispersions were shaken for 3 h, and the final

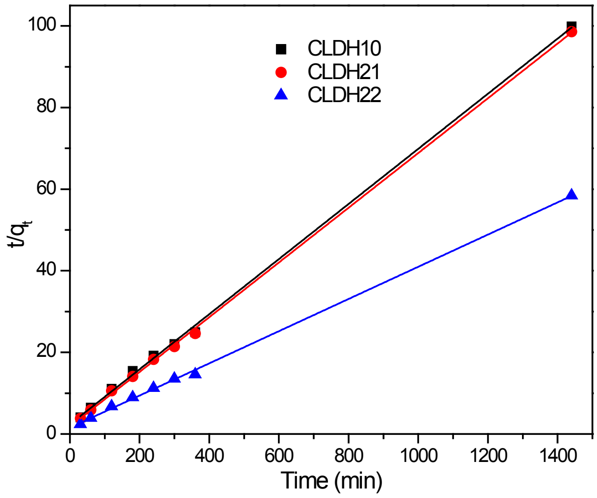

Fig. S8. The pseudo second order model of chromate anion sorption onto CLDHs plot.

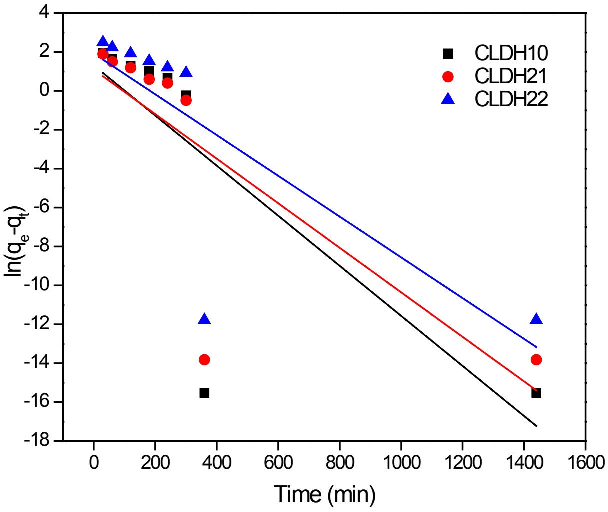

Fig. S7. The first order model of chromate anion sorption onto CLDHs plot.

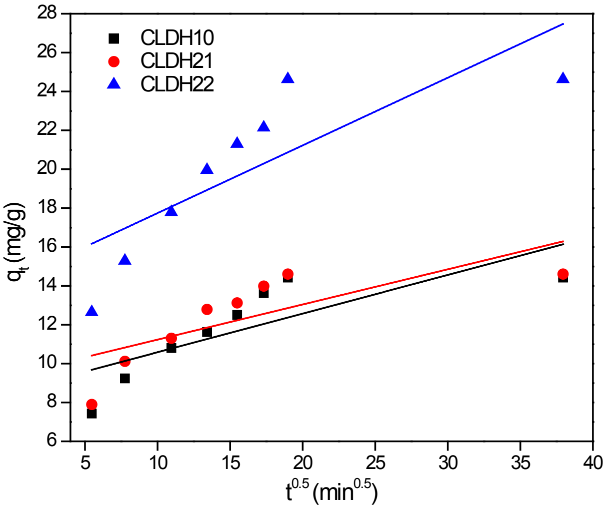

Fig. S9. The intraparticle diffusion model of chromate anion sorption onto CLDHs plot.

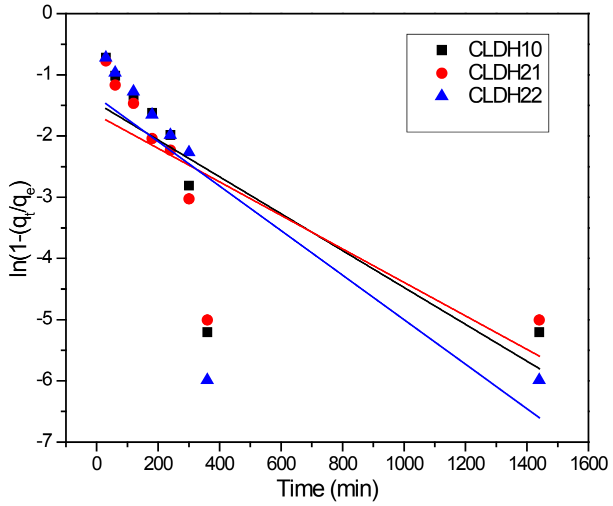

Fig. S10. The liquid film diffusion model of chromate anion sorption onto CLDHs plot.

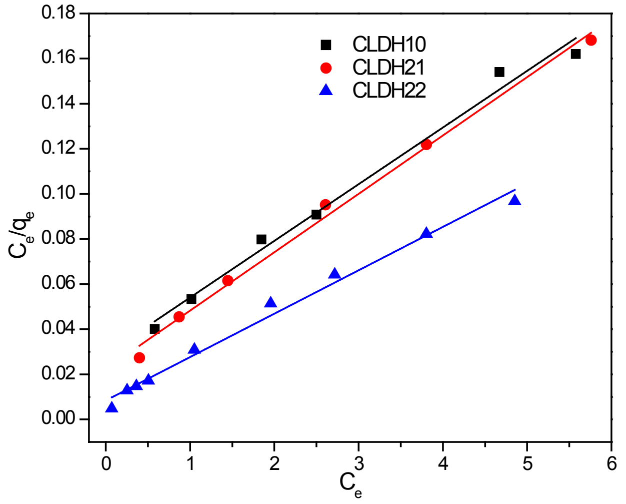

Fig. S11. Langmuir's isotherm sorption of chromate anion onto CLDHs sorbent plot.

pH of the solutions was measured. The pH_{PZC} was obtained from the intersection of the actual and theoretical graphs obtained by plotting initial and final pH values.

S4: Examination of kinetic models

The experimental sorption time data obtained was used in the four simplified kinetic equations form. The pseudo 1st order model can be described as in Eq. (1) [5]:

$$\ln(q_e - q_t) = \ln q_e - K_1 t \tag{1}$$

The pseudo 2nd order model can be described as in Eq. (2) [6]:

$$\frac{t}{q_t} = \frac{1}{K_2 q_e^2} + \frac{1}{q_e} t \tag{2}$$

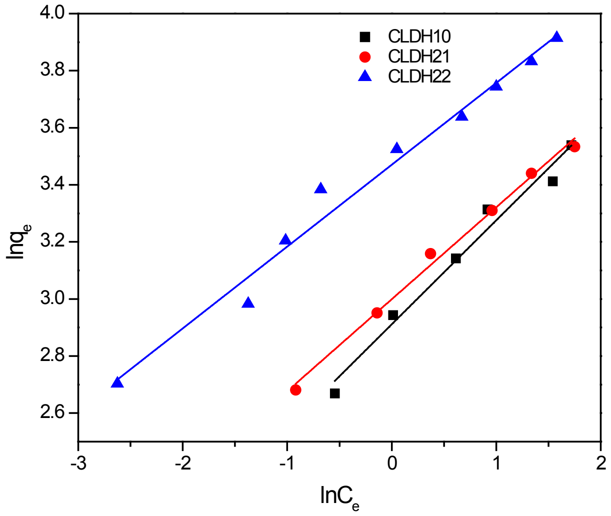

Fig. S12. Freundlich's isotherm sorption of chromate anion onto CLDHs sorbent plot.

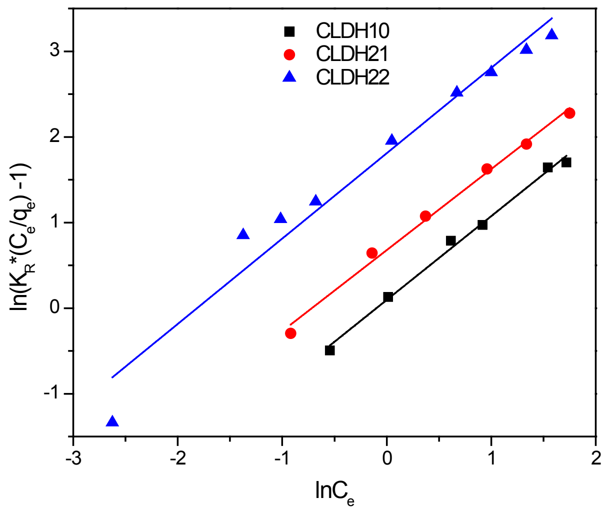

Fig. S13. Redlich-Peterson isotherm sorption of chromate anion onto CLDHs sorbent plot.

where, k_1, k_2 are the pseudo 1st (min^{-1}) and the pseudo 2nd order sorption ($g\ mg^{-1}\ min^{-1}$) rate constants, respectively; q_e and q_t represent the sorbed chromate amount ($mg\ g^{-1}$) at equilibrium and after time t (min), respectively.

The intraparticle diffusion rate model is expressed as shown in Eq. (3) [7]:

$$q_e = K_p \sqrt{t} + C \tag{3}$$

where, k_p is the rate constant intraparticle diffusion.

The liquid film diffusion model can be described as in Eq. (4) [8]:

$$\ln\left[1 - \frac{q_t}{q_e}\right] = R^1 t \tag{4}$$

where, R_1 (min^{-1}) is the liquid film diffusion constant.

S5: Fitting of sorption isotherm models

The most commonly utilized models applied for sorbent/sorbate systems for describing uptake isotherms are Langmuir's, Freundlich's and Redlich-Peterson equations.

Langmuir's isotherm model can be described as in Eq. (5) [9]:

$$\frac{C_e}{q_e} = \frac{1}{b_L q_{\max}} + \frac{C_e}{q_{\max}} \quad (5)$$

where, C_e is the concentration at equilibrium (mg L^{-1}), q_e and q_{max} are the amount sorbed at equilibrium (mg g^{-1}) and the greatest sorption capacity at monolayer coverage (mg g^{-1}), respectively and b_L is the constant of Langmuir's model referred to sorption energy (L mg^{-1}). The essential characteristics and the feasibility of Langmuir's isotherm can be described in a dimensionless equilibrium factor R_L term that is given by the following Eq. (6):

$$R_L = \frac{1}{1 + b_L C_\circ} \quad (6)$$

where, C_o is the initial concentration (mg L^{-1}), R_L value indicates that isotherm type is an irreversible ($R_L = 0$), favorable ($0 < R_L < 1$) or unfavorable ($R_L > 1$).

Freundlich's isotherm can be described by Eq. (7) [10]:

$$\ln q_e = \ln K_F + \frac{1}{n} \ln C_e \quad (7)$$

(K_F) is the Freundlich's constant model (d m^3 g^{-1}) and (*1/n*) is the sorption intensity.

Redlich-Peterson's isotherm can be described by Eq. (8) [11]:

$$\ln(\mathrm{K}_R \frac{C_e}{q_e} - 1) = \ln a_R + g \ln C_e \quad (8)$$

where, K_R and a_R (L/mg) are Redlisch–Peterson constants, g is an exponential value that lies between 0 and 1.

S6:Determination of the thermodynamic parameters

The thermodynamic parameters of sorption were calculated using Van't Hoff's Eq. (9):

$$\ln \mathrm{K}_d = \frac{\Delta S_{ads}}{R} - \frac{\Delta H_{ads}}{RT} \quad (9)$$

$$\Delta G_{ads} = \Delta H_{ads} - T\Delta S_{ads} \quad (10)$$

where, K_d is the distribution coefficient that equal to ($K_d = q_e/C_e$) and R is the molar gas constant (8.314 J mol^{-1} K^{-1}), ΔG_{ads}, ΔH_{ads} and ΔS_{ads} are the changes in sorption free energy, enthalpy and entropy, respectively.

References

[1] J. Mendham, R.C. Denney, J.D. Barnes, M. Thomas, B. Sivasankar, "Quantitative chemical analysis" sixth ed., Vogel's textbook, Pearson Education Ltd., New Delhi, India, (2000), pp. 58, 311–335, 349, 651, 70, 340.

[2] Z. Marczenko, Separation and spectrophotometeric determination of elements"; Ellis Horwood Limited, New York, second ed., 1986, pp. 21–43, 134.

[3] J. Mendham, R.C. Denney, J.D. Barnes, M. Thomas, B. Sivasankar, "Quantitative chemical analysis" sixth ed., Vogel's textbook, Pearson Education Ltd., New Delhi, India, (2000), pp. 58, 311–335, 349, 651, 70, 340.

[4] American Public Health Association (APHA), Standard method for examination of water and wastewater (20th edn). Washington: AWWA/WPCE. American Water Works Association, Water Environment Federation, (1999).

[5] S. Lagergren, B.K. Svenska, On the theory of so-called sorption of dissolved substances, K. Sven. vetensk. akad. handl., 24 (1898) 1–39.

[6] Y.S. Ho, G. McKay, Pseudo-second order model for sorption processes, Process Biochem., 34 (1999) 451–465.

[7] W. Weber, J.C. Morris, Kinetics of adsorption on carbon from solution, ASCE, 89 (1963) 31–60.

[8] G.E. Boyd, A.W. Adamson, L.S. Myers, The exchange adsorption of ions from aqueous solutions by organic zeolites, II, Kinetics. J. Am. Chem. Soc., 69 (1947) 2836–2848.

[9] I. Langmuir, The sorption of gases on plane surfaces of glass mica and platinum, J. Am. Chem. Soc., 40 (1918) 1361–1403.

[10] H.M.F. Freundlich, Over the sorption in solution, J. Phys. Chem., 57 (1906) 385–471.

[11] O. Redlich, D.L. Peterson, A useful adsorption isotherm, J. Phys. Chem., 63 (1959) 1024–1026.